Measurement of the Sea Spray Droplet Size Distributions at High Winds

William E. Asher
Applied Physics Laboratory, University of Washington
1013 NE 40th Street
Seattle, WA 98105
phone: (206) 543-5942 facsimile: (206) 543-6785 e-mail: asher@apl.washington.edu

C. W. Fairall
R/E/ET7
NOAA Environmental Technology Laboratory
325 Broadway
Boulder, CO 80305
Phone:303-497-3253 Fax: 303-497-6101 email: chris.fairall@noaa.gov

Award Number: N00014-02-1-0673
Award Number: N00014-02-1-0662 (DURIP)
http://www.apl.washington.edu

LONG-TERM GOALS

The long-term goal is to use a phase-Doppler anemometer (PDA) for measuring size-segregated droplet concentrations and fluxes at high wind speeds in the atmospheric boundary layer (ABL) in order to understand the dynamics of droplets at high wind speeds.

OBJECTIVES

Our objectives for FY 2005 were to complete the analysis of data from the Spray Production and Dynamics Experiment (SPANDEX) at the Water Research Laboratory at the University of New South Wales, analyze data collected using a PDA mounted in the NOAA aircraft N43RF during the 2004 hurricane season in Hurricane Jeanne, and complete the analysis of droplet size distributions measured using a high-speed video system during experiments conducted at the Air-Sea Interaction and Research Facility at NASA Wallops Flight Facility (WFF/ASIRF) .

APPROACH

At high wind speeds, droplets are injected upwards into the ABL by bursting bubbles and by shearing off of wave crests. These processes generate drops with radii that vary from a few tenths of a micrometer up to several hundred micrometers [*Andreas et al.*, 1995; *Resch and Afeti*, 1992; *Rossodivita and Andreussi*, 1999; *Spiel*, 1998; *Wu*, 1973]. Over this range, it is the droplets with sizes from a few tens of micrometers and larger that are believed to be important in the air-sea momentum and heat flux [*Kepert et al.*, 1999]. Of particular relevance to the CBLAST-Hurricanes study, sea spray has been proposed to have a large effect on the air-sea energy flux at hurricane-force wind speeds [*Andreas and Emmanuel*, 2001; *Perrie et al.*, 2005]. The fundamental parameter required for

Report Documentation Page

Form Approved
OMB No. 0704-0188

1. REPORT DATE **30 SEP 2005**	2. REPORT TYPE	3. DATES COVERED **00-00-2005 to 00-00-2005**

4. TITLE AND SUBTITLE **Measurement of the Sea Spray Droplet Size Distributions at High Winds**	5a. CONTRACT NUMBER
	5b. GRANT NUMBER
	5c. PROGRAM ELEMENT NUMBER
6. AUTHOR(S)	5d. PROJECT NUMBER
	5e. TASK NUMBER
	5f. WORK UNIT NUMBER
7. PERFORMING ORGANIZATION NAME(S) AND ADDRESS(ES) **University of Washington,Applied Physics Laboratory,1013 NE 40th Street,Seattle,WA,98105**	8. PERFORMING ORGANIZATION REPORT NUMBER
9. SPONSORING/MONITORING AGENCY NAME(S) AND ADDRESS(ES)	10. SPONSOR/MONITOR’S ACRONYM(S)
	11. SPONSOR/MONITOR’S REPORT NUMBER(S)

12. DISTRIBUTION/AVAILABILITY STATEMENT
Approved for public release; distribution unlimited

13. SUPPLEMENTARY NOTES
code 1 only

14. ABSTRACT
The long-term goal is to use a phase-Doppler anemometer (PDA) for measuring size-segregated droplet concentrations and fluxes at high wind speeds in the atmospheric boundary layer (ABL) in order to understand the dynamics of droplets at high wind speeds.

15. SUBJECT TERMS

16. SECURITY CLASSIFICATION OF:			17. LIMITATION OF ABSTRACT	18. NUMBER OF PAGES	19a. NAME OF RESPONSIBLE PERSON
a. REPORT **unclassified**	b. ABSTRACT **unclassified**	c. THIS PAGE **unclassified**	**Same as Report (SAR)**	**20**	

Standard Form 298 (Rev. 8-98)
Prescribed by ANSI Std Z39-18

characterizing these fluxes is the droplet source function, or number of droplets of a given size produced at the ocean surface per unit area and unit time. However, current instrumental techniques are unable to measure the source function directly, and it must be inferred from height-dependent droplet concentrations and a model for turbulent mixing in the atmosphere. Therefore, the droplet concentrations in the ABL required to estimate the source function implies measurement of particle concentrations over at least two orders of magnitude in size.

Droplet measuring instruments with the dynamic range in particle size required to measure droplet concentrations in the ABL have only recently become available. In order to provide two independent data sets for the droplet concentrations, a cloud imaging probe (CIP) (which measures size and concentration by imaging droplets) and a PDA (which measure size and velocity of individual droplets) were installed on the NOAA P-3 N43RF. The PDA was installed on the the NOAA aircraft N43RF in November of 2003 and was flight tested with the CIP in December 2003. It was ready for operation during the boundary layer profile measurements inside Hurricane Jeanne in September 2004 as part of the CBLAST hurricane research flights.

In similarity with a laser-Doppler velocimeter, a PDA measures the velocity of a moving particle by determining the Doppler shift in frequency of scattered light. However, a PDA also measures the particle size [*Asher and Farley*, 1995]. It uses the principle that when the same scattering event is viewed at two different locations, there is a phase difference, $\Delta\Phi$, between the two signals due to the difference in optical path to the detectors. Assuming the scattering geometry remains constant and the scattering particles are spherical, $\Delta\Phi$ is a function of particle radius, r, and the geometry of the scattering system [*Bauckhage et al.*, 1988]. Therefore, for a given scattering mechanism (e.g., first-order refraction) with a known system geometry (e.g., scattering angle, location of detectors) the relationship between $\Delta\Phi$ and r has a closed-form analytical expression [*Bauckhage et al.*, 1988] and measuring $\Delta\Phi$ allows calculation of r. It has been demonstrated that PDA systems accurately measure the number-size distributions of spherical particles in the submicron and supermicron size ranges [*Asher and Farley*, 1995; *Göbel et al.*, 1998; *Rossodivita and Andreussi*, 1999].

The research goal of the CBLAST flights were for the PDA and CIP to would provide size-segregated droplet concentrations as a function of aircraft altitude. These data sets could be intercompared and would then be used in a droplet boundary layer model such as formulated by *Kepert et al.* [1999] or *Pattison and Belcher* [1999] to determine the droplet source function. Once the source function is known, the contribution of droplets to surface exchange processes can be estimated.

One of the results of the field effort has been the recognition that measurement of the near-surface droplet flux in hurricanes is extremely challenging, taxing the personnel, measurement equipment and aircraft. Development of a remote sensing based technique to estimate droplet flux would be a major step forward. Therefore, we collaborated with Dr. William Plant of Applied Physics Laboratory (APL) in conducting a droplet flux study at WFF/ASIRF during March of 2004. A coherent Doppler radar measures droplet velocities and scattering intensities while droplet concentrations were measured using a high-speed video system. The data will be used to determine if Doppler radar cross sections can be used to infer droplet concentrations in the near-surface ABL.

WORK COMPLETED

The Spray Production and Dynamics Experiment (SPANDEX) at the Water Research Laboratory at the University of New South Wales (UNSW) was conducted in January and February of 2003. The data set from this experiment was used to investigate the dynamics of droplets produced through breaking waves and spray at high wind speeds. The PDA measured droplet sizes and their vertical and longitudinal horizontal velocities. In addition, a collocated wave height gauge gave water surface elevation at the PDA droplet sampling location. This provided a record of water surface elevation as a function of droplet size and speed.

In June of 2003, the engineering design, fabrication, and assembly of the mounting components required to install the PDA on the NOAA P-3 was begun. The installation was completed in November of 2003 with an initial instrument test flight in December of 2003. The PDA was made fully operational for the 2004 hurricane season and the CBLAST-Hurricane project research flights. Figure 1 shows the installation of the PDA on the P-3. It was mounted so that its sampling volume was outside the boundary layer of the aircraft but above the wing and slightly aft of the inboard propeller on the starboard side. This placement prevented using the vertical droplet velocities for any meaningful analysis since the droplet velocities were distorted by the flow over the wing. In 2004, the PDA was flown through both Hurricane Frances and Hurricane Jeanne. Instrumental problems prevented collecting any usable data in Frances but there were corrected in time to collect several days worth of data from Jeanne.

In March 2004, we conducted a laboratory spray droplet experiment at WFF/ASIRF wind-wave tunnel in collaboration with Dr. William Plant. These measurements provided initial data to be used as a proof-of-concept showing whether Doppler radar backscatter cross-sections can be used as a remotely-sensed indicator of spray droplet populations in the near-surface ABL. Size-segregated droplet concentrations in the facility were measured using a high-speed backlit microphotography system configured to detect droplets with radii in the range of 200 μm to 3000 μm. The PDA was not used in the WFF/ASIRF measurements because it was mounted on the P-3 and could not be removed and reinstalled in time for the hurricane season the coming fall. Droplet concentrations were measured as a function of height above the water surface for wind speeds up to 16 m s^{-1}. The concentration data will be compared to concentrations estimated from the radar backscatter cross-sections. The air-phase turbulence boundary layer was measured using a 3-transducer pitot-tube rake. The boundary layer measurements can be used with the droplet concentrations to estimate the droplet production at the water surface.

RESULTS

On of the main benefits of the PDA is that it provides two orthogonal components of the droplet velocity in addition to the droplet size. This allows the correlation of droplet size and velocity to be studied. These correlations are important in understanding how wave breaking generates the airborne droplets. Figure 2 is data from SPANDEX and shows histograms of water surface elevation for droplets measured at heights of 10 cm and 15 cm about the mean water surface. In both cases, the histogram is skewed to wave heights below the mean free surface, which means more droplets were

measured when the measurement volume was located over wave troughs than over wave crests. However, the skewness is larger for droplets measured at the higher height. This observation makes intuitive sense in that high speed video imagery suggests that droplets are produced at the wave crests and would be blown downwind to the measurement volume. Because it takes longer for droplets to rise to the upper measurement location, the droplets are measured farther downstream in relation to the wave crest.

The PDA data can also be used to study the correlation of particle size with velocity. Figure 3 shows the horizontal longitudinal (i.e., downstream) velocity of each drop plotted versus the droplet diameter for the data shown in Figure 2. Figure 4 shows the droplet vertical velocity plotted versus droplet diameter. The horizontal droplet velocities show a slight correlation with droplet diameter, with velocity decreasing slightly as droplet diameter increases. The vertical dashed lines in Figure 3 show the ranges over which the velocity was averaged. In the case of the data recorded at a height of 15 cm, the low diameter range was 0 μm to 30 μm and the high diameter range was 130 μm to 170 μm. For the 15 cm data, the average horizontal velocities for these two size ranges were 17.1 m s^{-1} and 15.4 m s^{-1}, respectively, showing that on average longitudinal velocity of the larger droplets was less than the velocity of the smaller droplets. In the case of the 10 cm height data, the smaller diameter range was the same but the larger diameter range was 90 μm to 130 μm and the respective average velocities were 13.4 m s^{-1} and 11.3 m s^{-1}. In contrast, there is no obvious correlation between drop size and vertical velocity, or between the horizontal and vertical velocities. Because of the small size of the droplets, the lack of correlation between vertical velocity and drop size is likely due to their their fall velocities being much less than the vertical turbulence velocities in the wind tunnel. One possible explanation for the correlation between horizontal velocity and droplet diameter would be that the droplets are accelerating off of the wave crests where they have been generated, and the larger droplets were measured before they had time to completely attain the free-stream flow velocity.

Figure 5 shows vertical air velocities and concurrent water surface elevations measured using small droplets seeded in the air flow generated by a spray gun located 2 m upwind of the PDA measurement volume in the wind-wave tunnel at UNSW during SPANDEX. The mean diameter of these droplets was approximately 20 μm and they could be assumed to track the air motions. There is a clear correlation between water surface elevation and the vertical air motions. This correlation can be used to infer the phase of the wave where droplets were likely to have been measured in Figures 2, 3, and 4. Because the average vertical velocity is negative in Figure 4, the data in Figure 5 suggest these droplets are measured over the upwind wave face, where the air motions are also in the negative direction.

The CIP was not available during the 2004 hurricane season. However, data are available from a test flight conducted in December of 2003 that allow intercomparison of rain droplet concentrations measured concurrently by the two instruments. Figure 6 shows rain drop concentrations measured by the CIP plotted along with drops measured by the PDA for two separate events measured during a test flight in December of 2003. There is very good agreement between the two instruments, suggesting both that the droplet populations were not severely affected by the presence of the propeller or flow distortion over the wing. Most importantly, the agreement shows that the PDA is able to make accurate measurements of droplet concentrations from an aircraft.

On September 22, 2004 the vertical gradient in spray droplet concentration was measured within Hurricane Jeanne using the stepped descent flight profile. Figure 7 is a plot of the flight track and altitude profile for the "figure 4" pattern and stepped descent flown on that day. The inset in the lower right corner of the flight track shows the detailed course of the stepped descent pattern. Also shown on the flight track as the darker segment crossing the center of the hurricane is a flight track for an eyewall penetration. Droplet concentrations from this flight track will be discussed below.

Figure 8 shows size-segregated droplet concentrations (i.e., the number of droplets of a given size range in a given volume of air) measured during the stepped descent in a cloud-free region between rain bands at altitudes of 708 m, 410 m, and 270 m. The droplet concentrations taken at the two higher altitudes show no significant difference, suggesting these were taken outside of the ABL where droplet concentrations were relatively constant with altitude. However, the concentrations at 270 m are significantly higher for droplets having diameters smaller than 120 μm. Because an altitude of 270 m is within the ABL, the increase in droplet concentration suggests that the PDA was able to measure the droplet concentration gradient. The similarity in concentrations for the larger droplets is due mainly to poor counting statistics and reflects the fact that for the larger drops at most two to three were counted in the larger size ranges. Unfortunately, the stepped descent had to be terminated at 270 m because of deteriorating visibility inside the storm. The aircraft was then out of service for the next two days having a chemical engine wash performed. Subsequent low-level flight operations were precluded when Jeanne became a land-falling storm and the aircraft was tasked with missions for the National Hurricane Center.

The bottom panel in Figure 9 shows a time series of droplet diameters measured along the eyewall penetration track shown in Figure 7 from the Sept. 22, 2004 flight in Hurricane Jeanne. The top panel in Figure 9 shows droplet concentrations averaged over three segments of the time series in the bottom panel. The first segment is for the initial eyewall penetration and spans 0 s to 100 s, the second spans 140 s to 280 s, and the third spans 310 s to 650 s. The time series and the concentration data show that there are essentially no droplets larger than 100 μm as the aircraft enters the eyewall clouds. After the aircraft has traveled approximately 8 km (assuming an average ground speed of approximately 100 m s^{-1}), the population of larger droplets increases and remains relatively constant through the body of the storm.

Figure 10 shows a flight track and altitude/longitude plot similar to Figure 7 except it is from the flight into Hurricane Jeanne on Sept. 25, 2004. The eyewall penetration segment is shown as the darker portion of the flight track. Figure 11 shows a droplet diameter time series and droplet concentration plot for the eyewall penetration from the Sept. 25 data set. As was seen in the eyewall penetration droplet data from the flight on Sept. 22, the concentration of droplets larger than 100 μm is much lower compared with data taken further away from the center of the storm. Although not shown because of space limitations, this effect was observed on several other eyewall penetration data sets from flights on Sept. 22, Sept. 24, and Sept. 25.

Figure 12 shows droplet concentrations measured at a wind speed of 16 m s^{-1} at heights of 11.5 cm, 14.0 cm, 16.5 cm, and 19.0 cm. As expected, the concentrations decrease with height above the mean

water surface. Further analysis of this data will be performed once the radar data have been completely analyzed.

IMPACT/IMPLICATION

The PDA has been shown to be an effective instrument for aircraft-based airborne droplet measurements. In this sense the research performed here was a large success because a new tool is available to researchers interested in studying atmospheric aerosols. The remote sensing study conducted at WFF will provide a proof-of-concept result on using coherent radar to remotely measure droplet concentrations in the near-surface marine boundary layer.

REFERENCES

Andreas, E.L., J.B. Edson, E.C. Monahan, M.P. Rouault, and S.D. Smith, The spray contribution to net evaporation from the sea: A review of recent progress, *Bound.-Layer Meteor.*, *72*, 3-52, 1995.

Andreas, E.L., and K.A. Emmanuel, Effects of sea spray on tropical cyclone intensity, *J. Atm. Sci.*, *58*, 3741-3751, 2001.

Asher, W.E., and P.J. Farley, Phase-Doppler anemometer measurement of bubble concentrations in laboratory-simulated breaking waves, *J. Geophys. Res.*, *100*, 7045-7056, 1995.

Bauckhage, K., H.H. Floegel, U. Fritsching, and R. Hiller, The phase-Doppler difference method, a new laser-Doppler technique for simultaneous size and velocity measurements. Part 2: optical particle characteristics as a base for the new diagnostic technique, *Part. and Part. Syst. Charac.*, *5*, 66-71, 1988.

Göbel, G., T. Wriedt, and K. Bauckhage, Micron and submicron aerosol sizing with a standard phase-Doppler anemometer, *J. Aerosol Sci.*, *29* (9), 1063-1073, 1998.

Kepert, J.D., C.W. Fairall, and J.-W. Bao, Modelling the interaction between the atmospheric boundary layer and evaporating sea spray droplets, in *Air-Sea Fluxes of Momentum, Heat and Chemicals*, edited by G. Geernaert, Kluwer Academic Publishers, Norwell, 1999.

Pattison, M.J., and S.E. Belcher, Production rates of sea-spray droplets, *J. Geophys. Res.*, *104*, 18,397-18,407, 1999.

Perrie, W., E.L. Andreas, W. Zhang, W. Li, J. Gyakum, and R. McTaggart-Cowan, Sea spray impacts on intensifying midlatitude cyclones, *J. Atm. Sci.*, *62*, 1867-1883, 2005.

Resch, F., and G. Afeti, Submicron film drop production by bubbles in seawater, *J. Geophys. Res.*, *97C*, 3679-3683, 1992.

Rossodivita, A., and P. Andreussi, Spray production by air bubbles bursting on a water surface, *J. Geophys. Res.*, *104* (C12), 30059-30066, 1999.

Spiel, D.E., On the birth of film drops from bubbles bursting on seawater surfaces, *J. Geophys. Res.*, *103C*, 24,907-24,918, 1998.

Wu, J., Spray in the atmospheric surface layer: Laboratory study, *J. Geophys. Res.*, *78*, 511-519, 1973.

PUBLICATIONS

Asher, W.E., and T. Litchendorf, 2005: "The use of a phase-Doppler anemometer to measure droplet populations in the marine boundary layer," *J. Atm. Ocean. Tech.*, in preparation.

Plant, W.J., W.C Keller, and W.E. Asher, 2006: "Is Sea Spray a Factor in Microwave Backscatter from the Ocean?," submitted to 9th Specialist Meeting on Microwave Radiometry and Remote Sensing Applications, San Juan, Puerto Rico, 28 Feb. 2006 through 3 March 2006.

Figure 1: Photographs showing the installation of the phase-Doppler anemometer on the NOAA P-3 N43RF (Miss Piggy). Left image shows electronics (beige box in lowest left shelf of rack, laser power supply and frequency converter (black boxes in lowest right shelf), data acquisition computer (notebook computer on tray in the middle of the rack on the left side), and laser and fiber optic coupler (black boxes mounted on aluminum rail on top of the rack) as mounted in the rack at station C3X. The right image shows the transmitting (lower cylindrical object on vertical mounting post) and receiving optics (upper cylinder on post) mounted to look out the window at station C7.

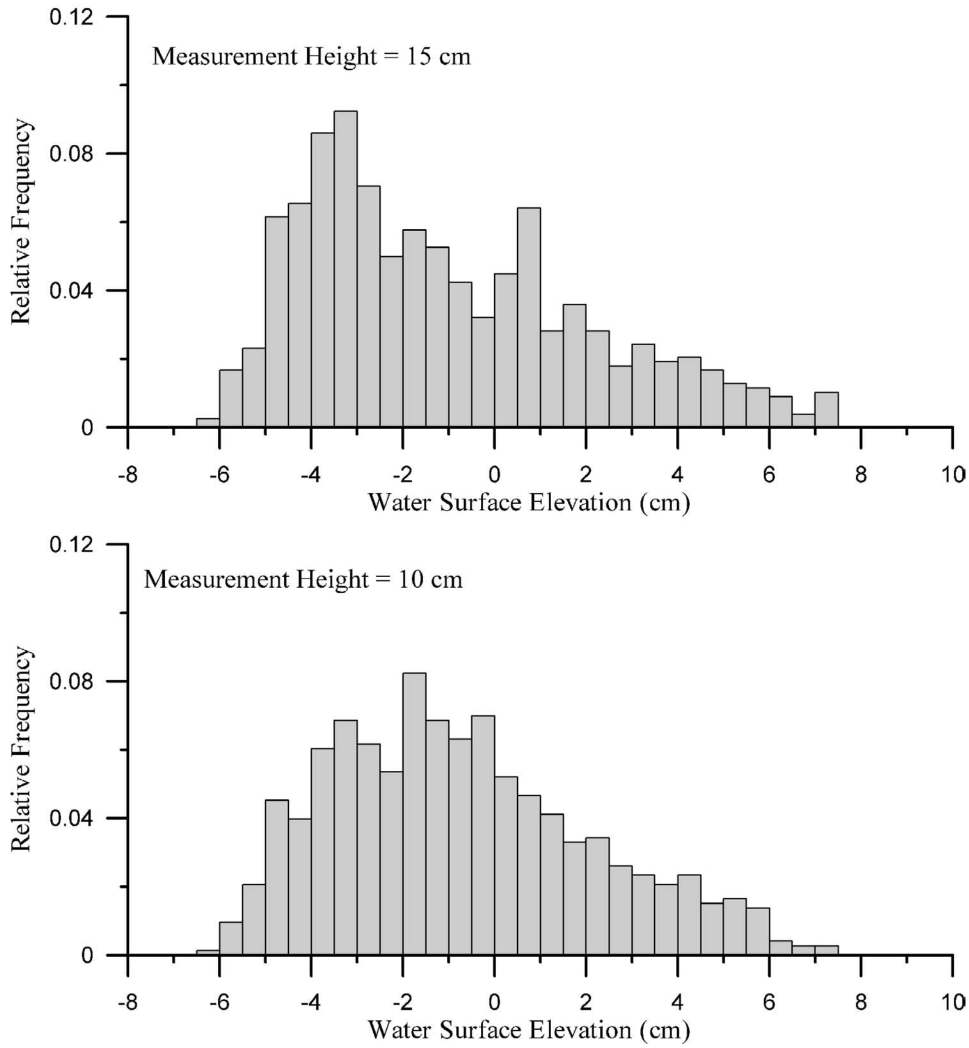

Figure 2: Two histograms of the water surface elevation measured under each droplet detected during two 30-minute data runs during the Spray Droplet and Dynamics Experiment conducted in February of 2003 at the University of New South Wales Water Research Laboratory. The show that droplets were more likely to be detected over wave troughs than crests, suggesting the droplets are produced at the crests and are blown out over the troughs. The top histogram shows water elevations for droplets measured 15 cm above the mean water surface and the bottom histogram is for droplets measured 10 cm above the mean water surface. The skew is larger for the higher elevation since droplets take longer to rise to the higher elevation.

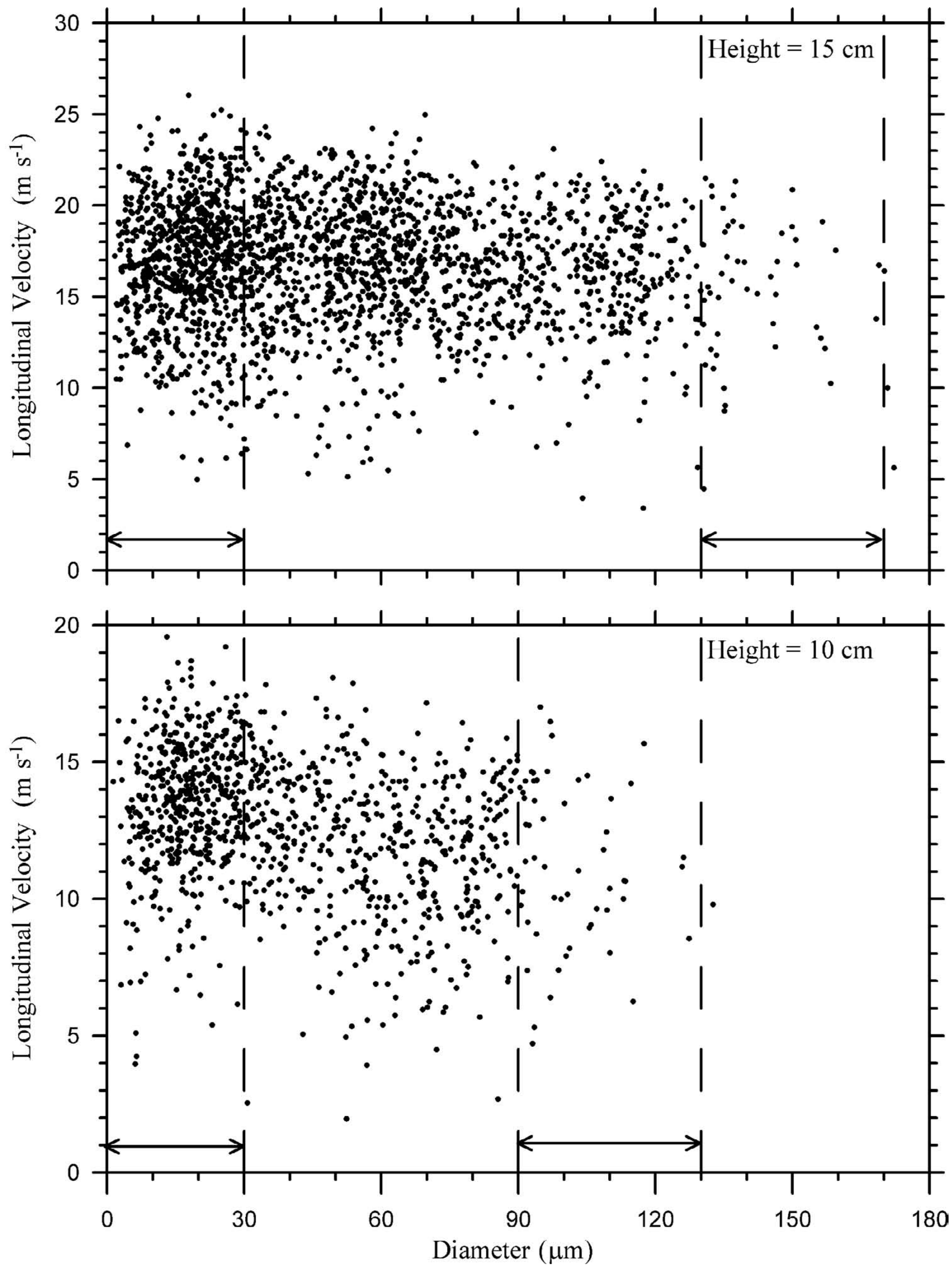

Figure 3: Two plots of droplet longitudinal horizontal (i.e., downwind) velocities measured during the Spray Droplet and Dynamics Experiment in February of 2003 at the University of New South Wales Water Research Laboratory. Velocity and diameter were measured simultaneously using a phase-Doppler anemometer (PDA). The upper plot shows droplets measured at an elevation of 15 cm above the mean water surface. The lower plot shows droplets measured at an elevation of 10 cm. The vertical dashed lines in each figure show the range of droplet sizes over which average longitudinal velocities were computed. The data show the trend of decreasing longitudinal velocity as droplet diameter increases.

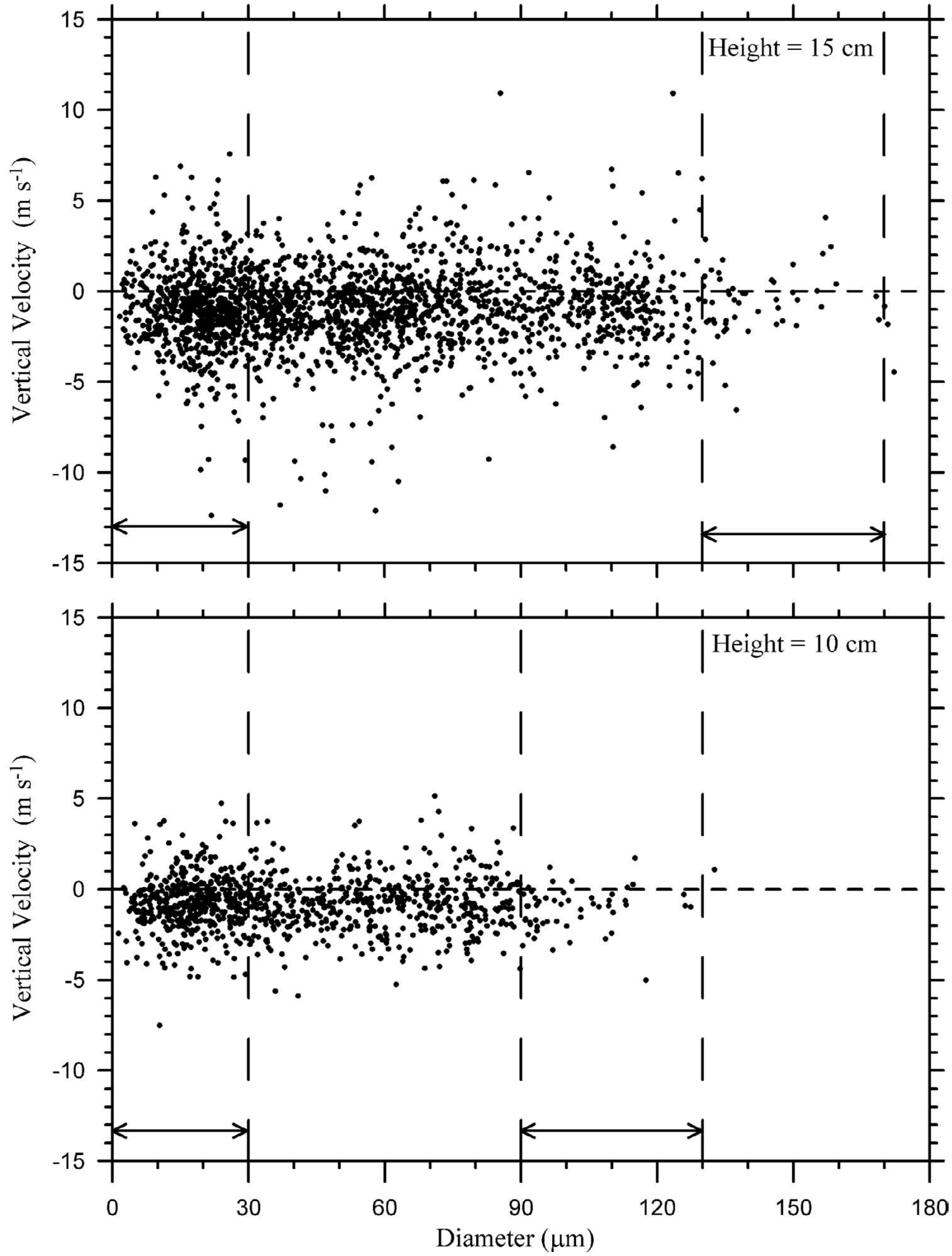

Figure 4: Two plots of droplet vertical velocities measured during the Spray Droplet and Dynamics Experiment in February of 2003 at the University of New South Wales Water Research Laboratory. Velocity and diameter were measured simultaneously using a phase-Doppler anemometer (PDA) and the data sets are the same as shown in Figure 3. The upper plot shows droplets measured at an elevation of 15 cm above the mean water surface. The lower plot shows droplets measured at an elevation of 10 cm. The vertical dashed lines in each figure show the range of droplet sizes over which average vertical velocities were computed. The data show there is no significant correlation between vertical velocity and droplet diameter.

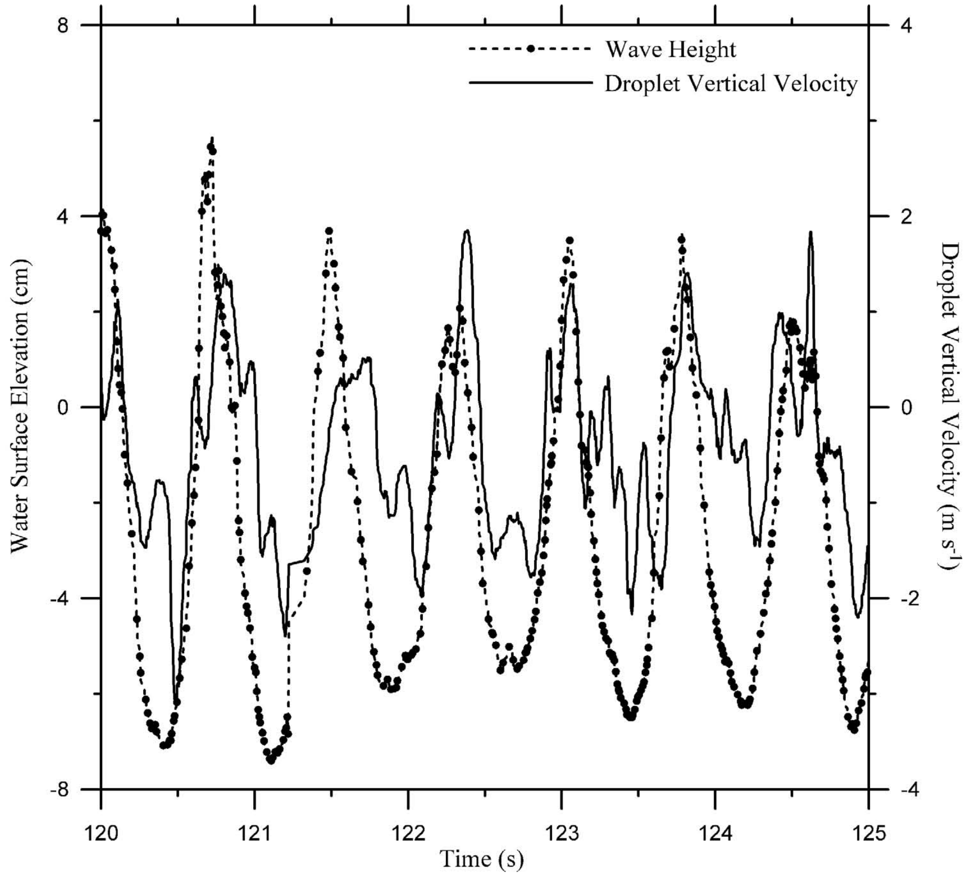

Figure 5: Time series of vertical velocities measured in the wind-wave tunnel at University of New South Wales Water Research Laboratory during the Spray Production and Dynamics Experiment. The velocities were measured using droplets seeded using a paint sprayer located 2 m upwind of the phase-Doppler anemometer sampling point. The data show that there is a correlation between water surface elevation and vertical air motion above the water.

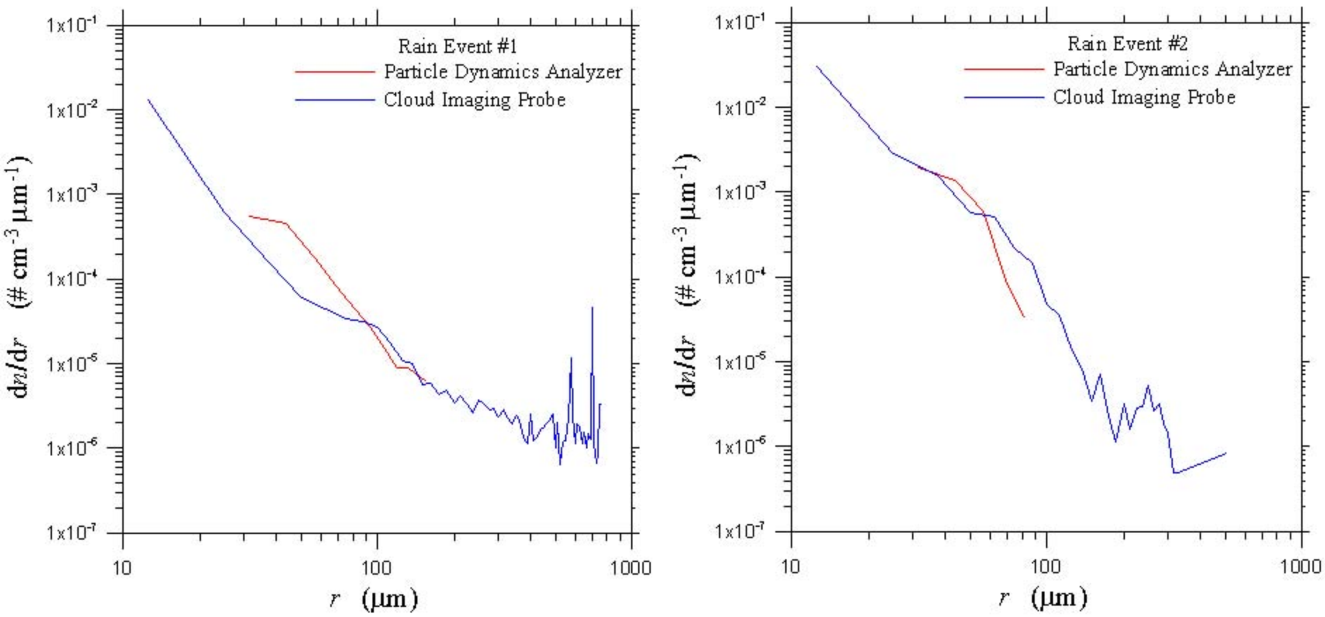

Figure 6: Two plots of airborne droplet concentrations (represented as number of drops per micron of radius per cubic centimeter of volume) in two different rain events measured using the Cloud Imaging Probe (CIP) and phase-Doppler anemometer (PDA) aboard the NOAA P-3 N43RF in December, 2003. There is good agreement between the concentrations measured by the CIP and the PDA.

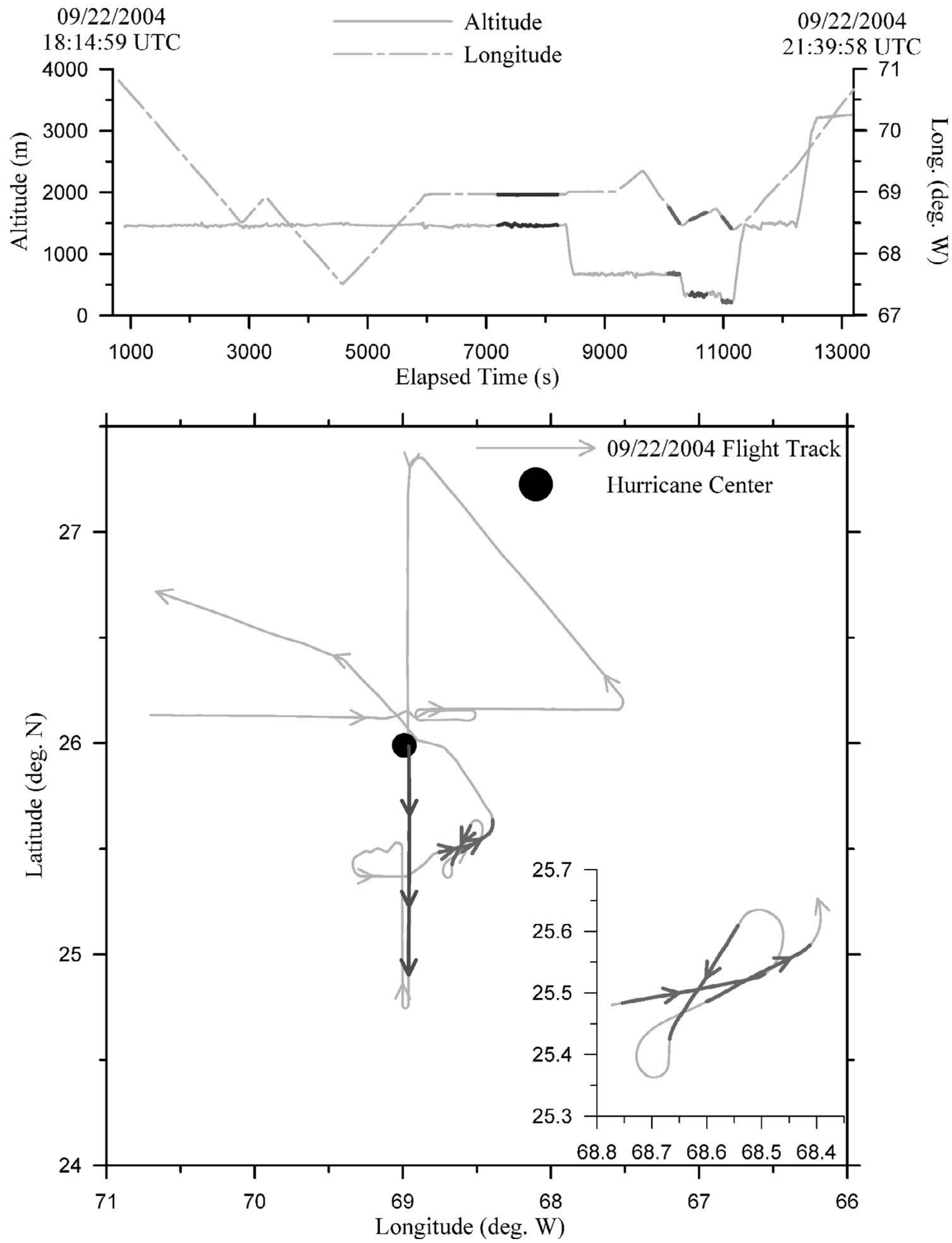

Figure 7: Flight level and position data of NOAA P-3 N43RF in Hurricane Jeanne on September 22, 2004. The top panel shows a time series of aircraft altitude and longitude. The bottom panel shows the aircraft position and direction in the "figure 4" flight pattern, the location of the stepped descent pattern relative to the storm center, the eyewall penetration track, and the inset in the lower right corner shows the detailed flight track of the stepped descent pattern.

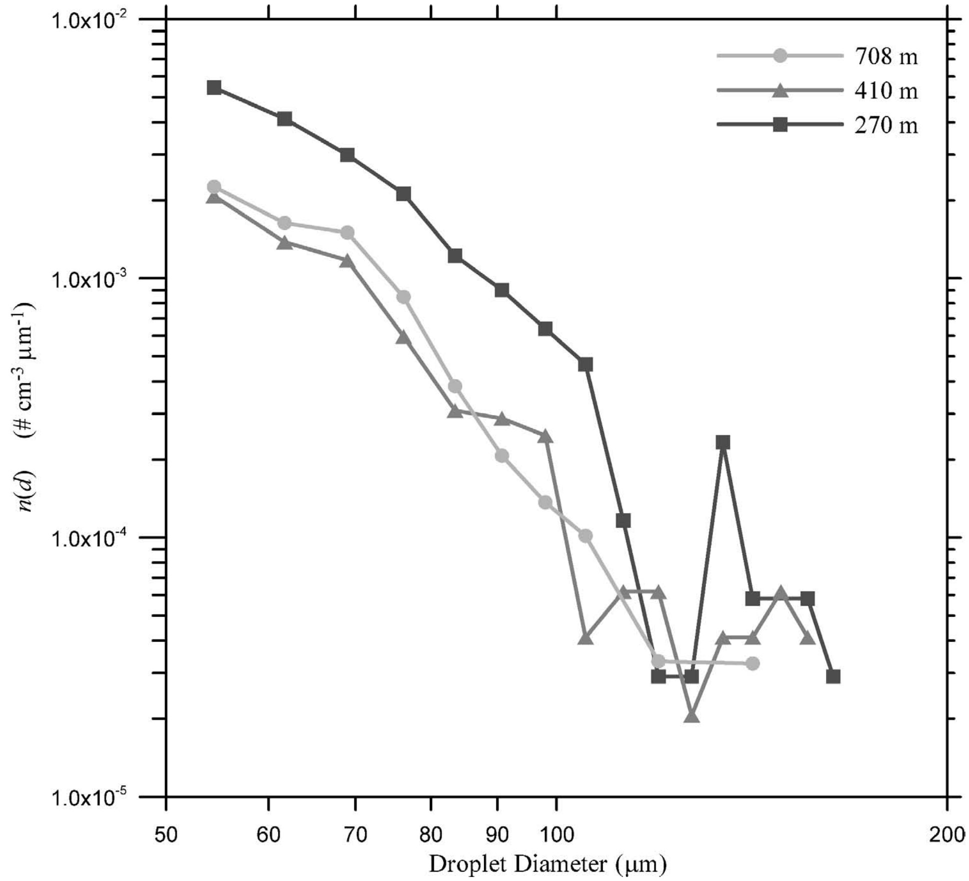

Figure 8: A plot of size segregated spray droplet concentrations (i.e., number of droplets in a given size range per volume of air) in a cloud-free area as a function of aircraft altitude for data taken with the phase-Doppler anemometer in Hurricane Jeanne on September 22, 2004 at altitudes of 708 m, 410 m, and 270 m. Droplet concentrations are essentially equal for the two higher altitudes and then increase with decreasing measurement height.

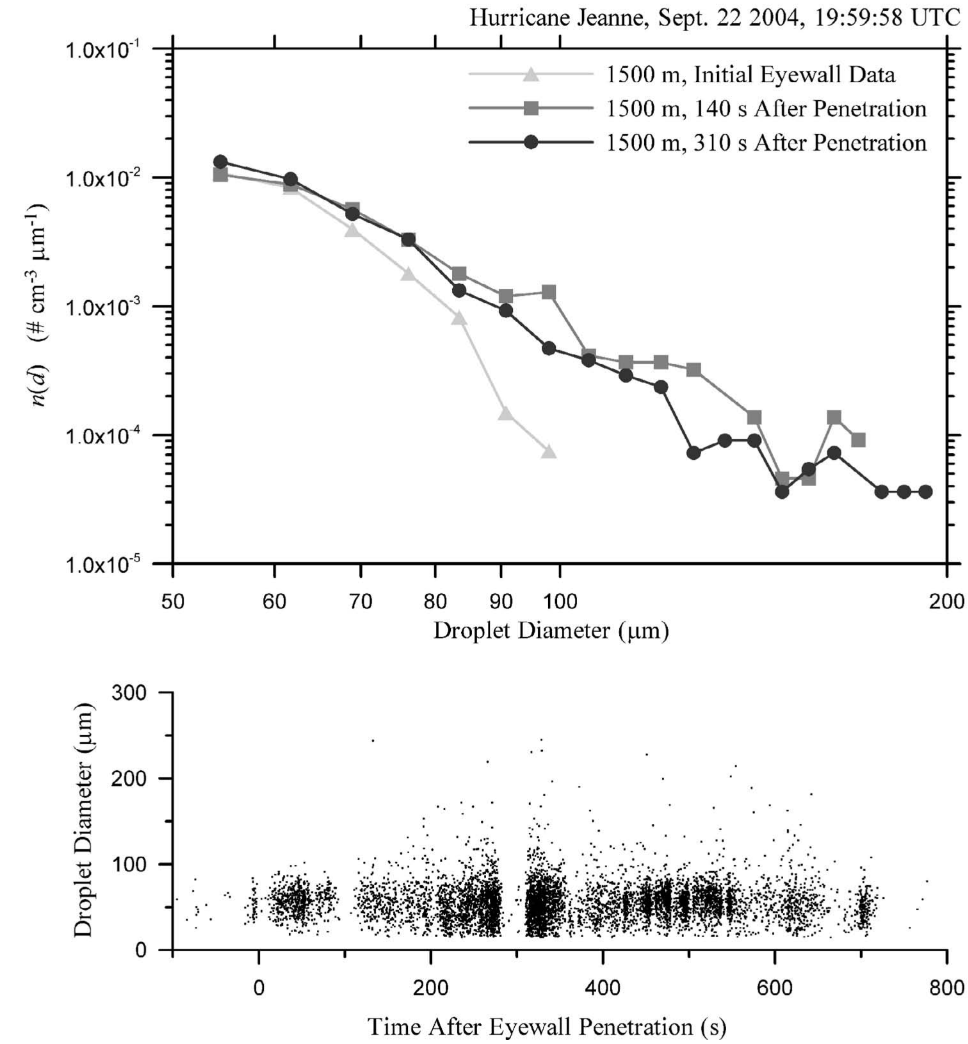

Figure 9: Cloud and rain droplet populations for a flight track from the eye of Hurricane Jeanne outwards, penetrating the eyewall on September 22, 2004. The top plot shows size segregated droplet concentrations (i.e., number of droplets in a given size range per volume of air) for three time intervals along the eyewall penetration flight track shown in Figure 7. The bottom plot is a time series of droplet diameter for the same eyewall penetration track on Sept. 22. The data show that the average droplet size is smaller during the first part of the eyewall penetration.

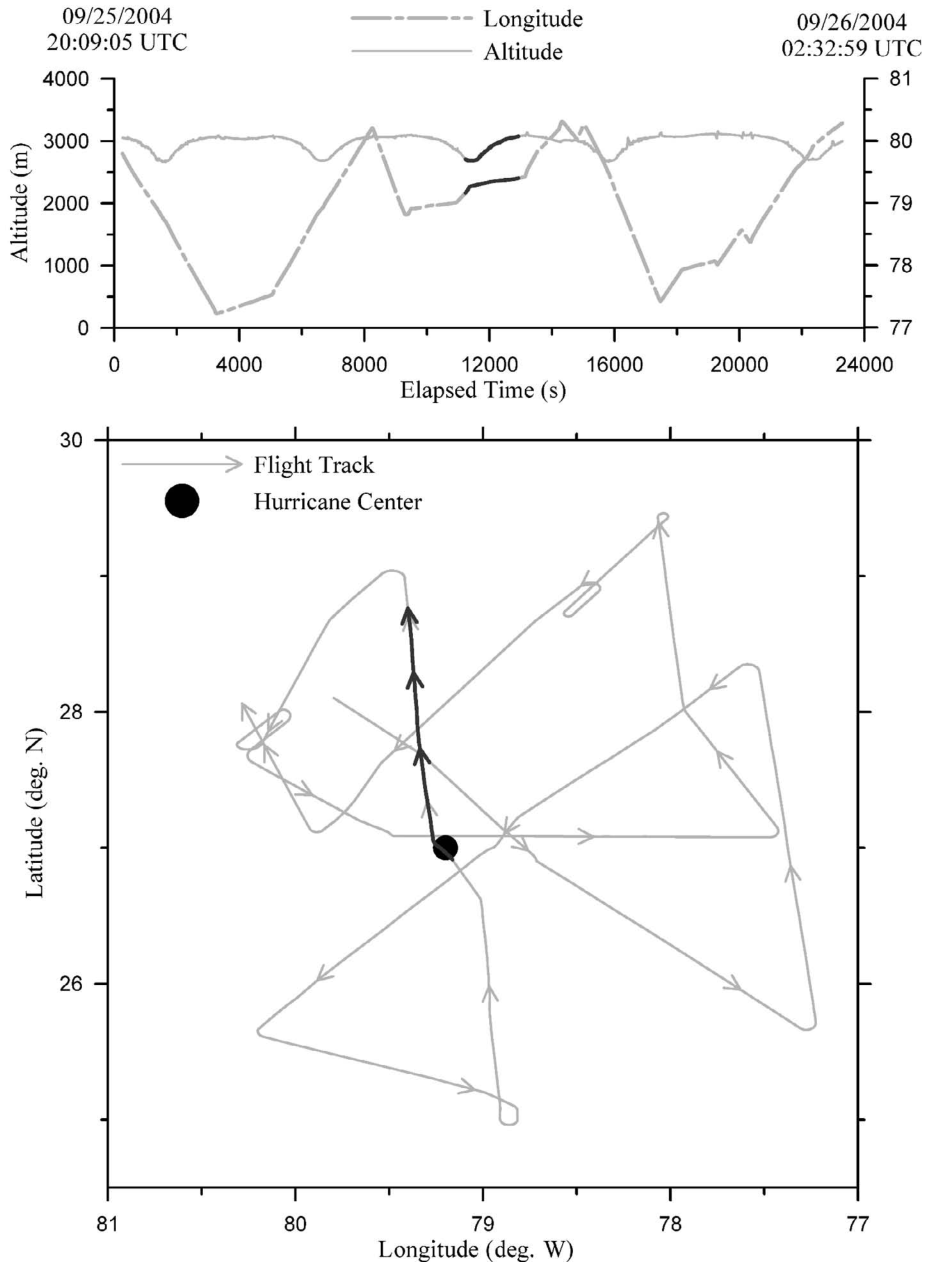

Figure 10: Flight level and position data of NOAA P-3 N43RF in Hurricane Jeanne on September 25, 2004. The top panel shows a time series of aircraft altitude and longitude. The bottom panel shows the aircraft position and direction in the "figure 4" flight pattern and the eyewall penetration track.

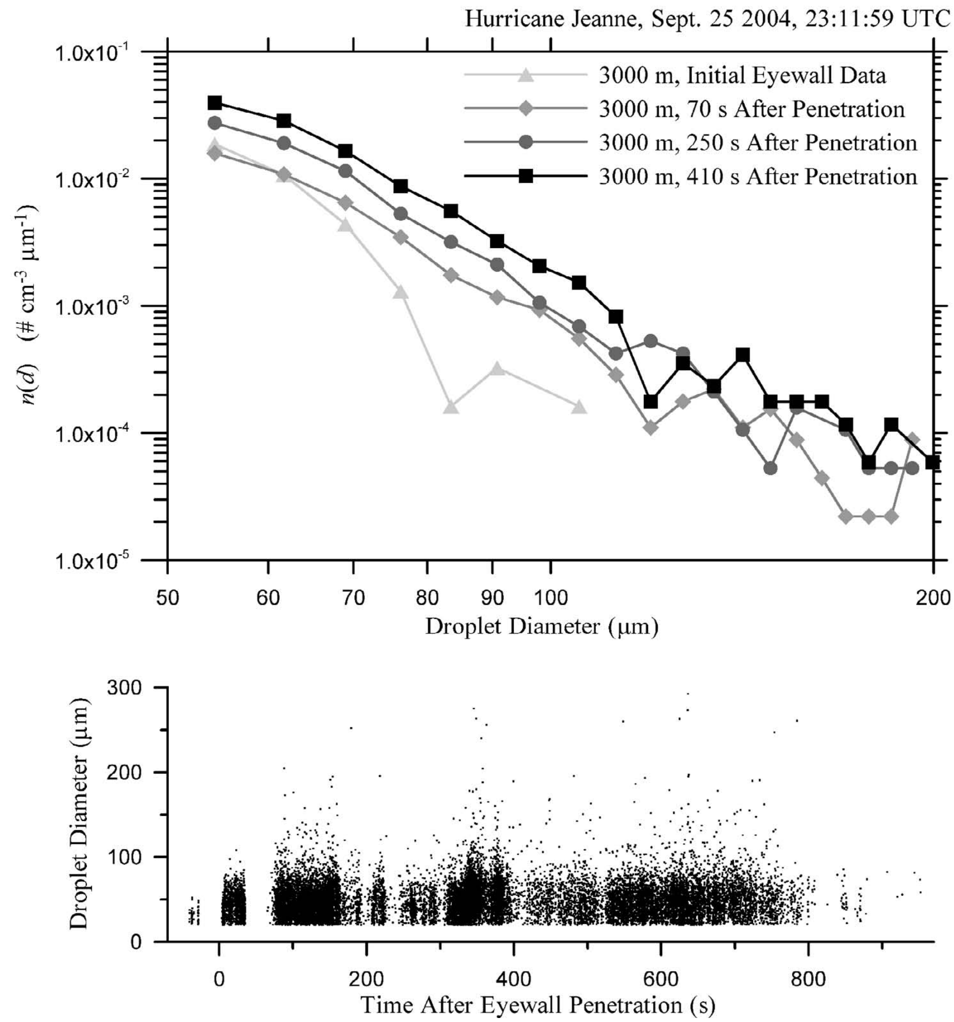

Figure 11: Cloud and rain droplet populations for a flight track from the eye of Hurricane Jeanne outwards, penetrating the eyewall on September 25, 2004. The top plot shows size segregated droplet concentrations (i.e., number of droplets in a given size range per volume of air) for four time intervals along the eyewall penetration flight track shown in Figure 10. The bottom plot is a time series of droplet diameter for the same eyewall penetration track on Sept. 25. The data show that the average droplet size is smaller during the first part of the eyewall penetration.

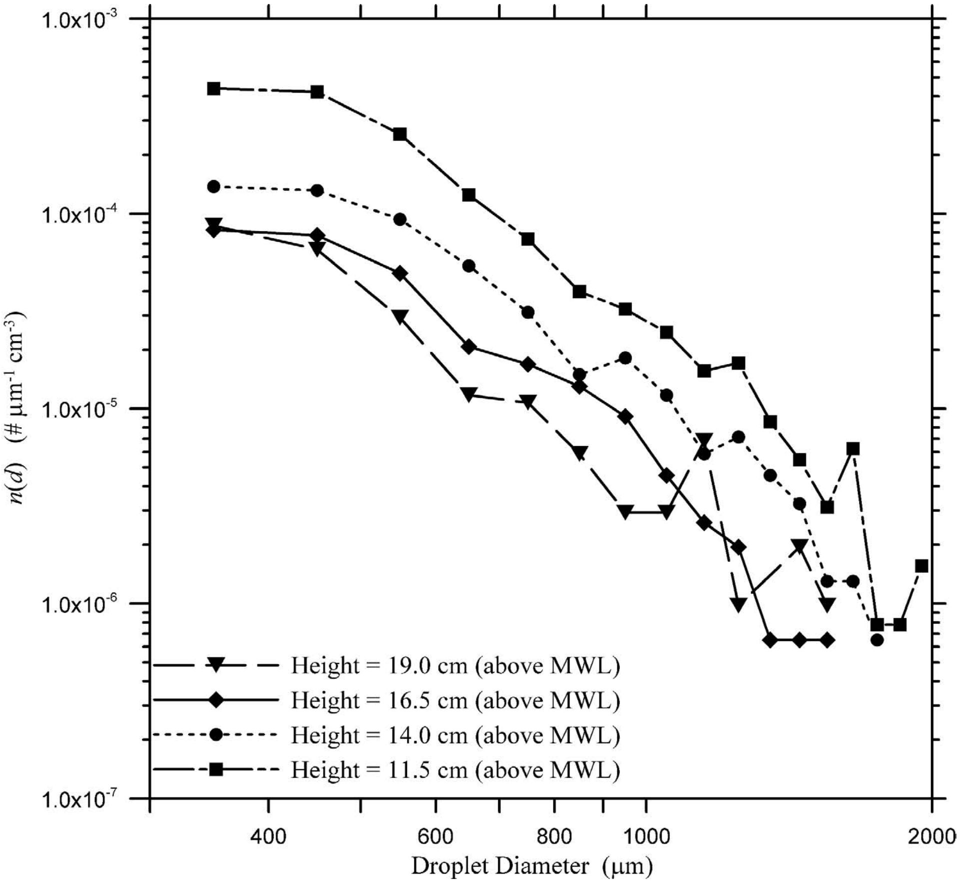

Figure 12: A plot of size segregated droplet concentration (i.e., number of droplets in a given size range per volume of air) as a function of height at a wind speed of 16 m s^{-1} as measured using a high-speed video system during the coherent radar spray study conducted at NASA Wallops Flight Facility. The data show that droplet concentrations increase as measurement height decreases.